Nanoscale Res Lett (2009) 4:635–639
DOI 10.1007/s11671-009-9287-9

NANO EXPRESS

Monitoring Charge Exchange in P3HT-Nanotube Composites Using Optical and Electrical Characterisation

Ioannis Alexandrou · Emmanouil Lioudakis · Dimitrios Delaportas · C. Z. Zhao · Andreas Othonos

Received: 16 September 2008 / Accepted: 5 March 2009 / Published online: 19 March 2009

Abstract Charge exchange at the bulk heterojunctions of composites made by mixing single wall nanotubes (SWNTs) and polymers show potential for use in optoelectronic devices such as solar cells and optical sensors. The density/total area of these heterojunctions is expected to increase with increasing SWNT concentration but the efficiency of solar cell peaks at low SWNT concentrations. Most researchers use current–voltage measurements to determine the evolution of the SWNT percolation network and optical absorption measurements to monitor the spectral response of the composites. However, these methods do not provide a detailed account of carrier transport at the concentrations of interest; i.e., near or below the percolation threshold. In this article, we show that capacitance–voltage (C–V) response of (metal)-(oxide)-(semiconducting composite) devices can be used to fill this gap in studying bulk heterojunctions. In an approach where we combine optical absorption methods with C–V measurements we can acquire a unified optoelectronic response from P3HT-SWNT composites. This methodology can become an important tool for optoelectronic device optimization.

I. Alexandrou (✉) · D. Delaportas · C. Z. Zhao
Electrical Engineering and Electronics, University of Liverpool, Liverpool L69 3GJ, UK
e-mail: ioannis@liv.ac.uk

E. Lioudakis · A. Othonos
Department of Physics, Research Center of Ultrafast Science, University of Cyprus, P.O. Box 20537, Nicosia 1678, Cyprus

E. Lioudakis
Energy, Environment and Water Research Center, The Cyprus Institute, P.O. Box 27456, Nicosia 1645, Cyprus

Introduction

Composites of polymers and nanotubes have attracted much attention lately because they are lightweight, relatively simple to fabricate, and are a low cost alternative to current structural and electronic materials. In mechanical applications nanotubes are used to increase the stiffness and toughness of the host polymer [1] with much research on dispersion methodologies [2, 3] and the mechanical behavior of nanotubes and their arrays [4]. Polymer–nanotube electronic materials on the other hand are set to explore the charge exchange at the polymer–nanotube heterojunctions within the volume of the composite. Optoelectronic characterization such as photoluminescence [5, 6] optoelectronic memory effect [7], and photovoltaic response [8–16] suggest that nanotubes act as electron donors to the polymer host. Even though the mechanical properties of composites improve by increasing the nanotube concentration, the electronic response is usually optimum for low concentrations of nanotubes [11, 14, 17]; usually close to the percolation threshold.

In this article we use two different methodologies to probe the interaction between poly (3-hexylthiophene), (P3HT), and single wall nanotubes (SWNTs) and probe the charge exchange at their heterojunctions. Optical linear absorption and femtosecond transient absorption measurements are then used to study P3HT–SWNT composites at high SWNT concentrations. Electrical capacitance–voltage measurements of metal-oxide-semiconductor (MOS) devices are then used to monitor charge exchange at SWNT concentrations near or below the percolation limit. Our results show that this combination of optical and electrical methods provide a useful tool for studying charge exchange in polymer–nanotube composites over a wide

range of SWNT concentrations and therefore can help to optimize their optoelectronic response.

Experimental

Composites of P3HT and SWNTs were prepared by mixing appropriate amounts of the two materials dissolved in 1,2-dichlorobenzene. SWNTs were obtained from CNI (research grade purified Hipco SWNTs) and were used without further functionalization. The composite solution was then sonicated further until it was homogeneous. Layers of the composite were drop cast on the substrate: quartz discs for optical measurements; n^+Si with 200 nm thick thermally grown SiO_2 for capacitance–voltage (*C–V*) measurements; glass for conductivity measurements. The inset in Fig. 3 shows the geometry of the devices used for *C–V* and *I–V* measurements. The heavily doped n^+Si with evaporated Al back contact serves as the gate during *C–V* testing. All samples were dried in air overnight and then were kept in vacuum for at least 12 h to ensure full drying of the solvent. The Au top contacts for *C–V* and *I–V* measurements were subsequently deposited by evaporation. The Au contacts for *C–V* were 1 mm dots while for *I–V* we used 200 × 200 μm square contacts at 50 μ m from each other. The *C–V*, *I–V*, and optical measurements were performed in air. The ramp rate during *C–V* measurements was 1 V/s and the peak-to-peak value of the probing voltage was 50 mV.

For the time resolved measurements we have used a non collinear super-continuum pump probe configuration in conjunction with a regenerative Ti:Sapphire amplifier system producing 100 fs pulses at 800 nm. The temporal resolution of the system has been measured to be better than 150 fs. In this work, optical pumping at a fluence of 2 mJ/cm^2 was used to excite the composites and determine their temporal behaviour. Here, we should point out that around this fluence non linear effects such as exciton–exciton annihilation were not observed in our experimental studies. More details on sample preparation and details of our optical system can be found in a recent publication [18].

Results and Discussion

Figure 1 shows the absorption spectra for the pure P3HT polymer and three of its composites with SWNTs. As the nanotube concentration increases, the composite solution becomes thinner. Since our samples have been prepared by drop casting similar amounts of the composite solution on the substrate, films of composites with high SWNT (<20 wt%) concentrations are visibly thinner. This affects

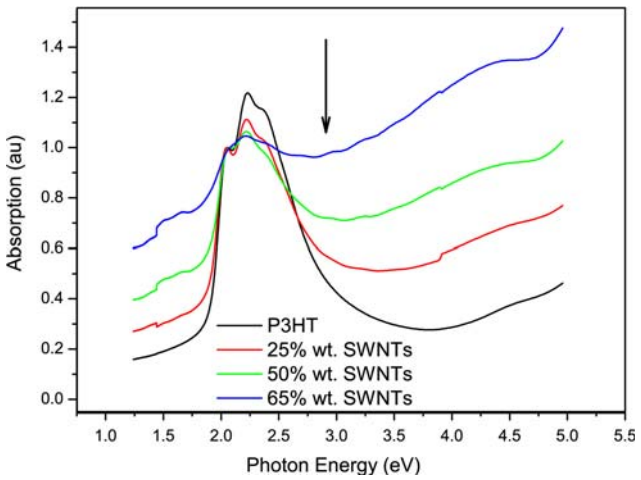

Fig. 1 Absorption spectra for P3HT–SWNT composites of various concentrations. All spectra have been scaled to the 2. eV peak to allow for decreasing film thickness with increasing SWNT concentration. The vertical arrow indicates the energy of the pump beam photons in pump–probe measurements shown in Fig. 2

the absorption measured and we have therefore scaled all curves in Fig. 1 so as all 2.1 eV peaks have the same amplitude, similar to other reports in the literature [19]. As a result we can safely compare the shape of the curves to reveal structural characteristics but comparison of absolute values requires careful attention. The main absorption in the energy range studied here comes mainly from the polymer but the fine structure in the absorption curves between 2.1 and 2.4 eV disappears progressively as the nanotube concentration increases. This change in absorption shows that the structure of the polymer is interrupted by the incorporation of the nanotubes. According to recent reports, the structure of the polymer can be strongly modified at nanotube concentrations as low as 1 wt% [20–22]. In these references, the composite preparation involves particular steps to stimulate P3HT crystallization on the nanotube walls. In our case the simple mixing of P3HT and SWNTs reveal the same trend albeit at higher SWNT concentrations. However, we do not expect to affect the regioregularity and thus the basic properties of P3HT.

In order to monitor the behavior of excited carriers in these composites we have used the non collinear pump–probe technique. In this method, the absorption change of the material is continuously monitored at some pre-selected wavelengths. An ultrashort laser pulse (pump) is used to excite the carriers in the material and a second weak pulse is used to follow the change in absorption immediately afterwards with femtosecond resolution [23]. Figure 2 shows transient absorption measurements for the pure P3HT polymer and P3HT/SWNT composites at a probing wavelength of 600 nm (2 eV). According to the linear absorption spectra of Fig. 1 using this wavelength we are

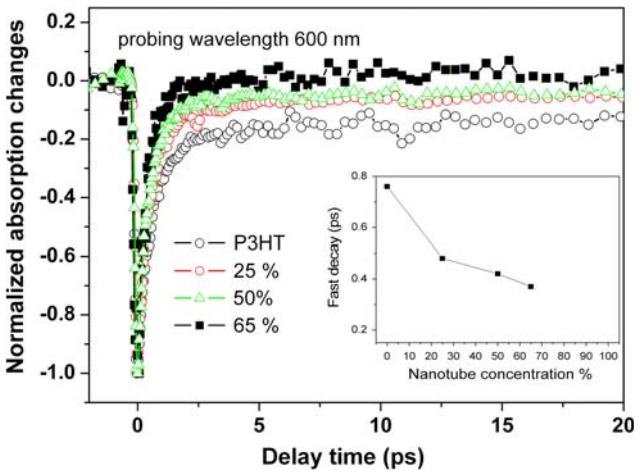

Fig. 2 Normalized transient absorption measurements for the P3HT polymer and SWNT/P3HT composites at probing wavelength of 600 nm. The inset shows the time constant of the fast absorption decay as a function of nanotube concentration

probing absorption from the HOMO to states at the bottom of the LUMO in P3HT. The initial excitation by the pump pulse (3.1 eV) is immediately followed by a sharp decline in absorption by the material. This is a direct consequence of the monitored states being filled up by relaxing excitons created by the pump pulse. Following this initial 'state filling' the excitons relax further and the population of empty states 2 eV above the HOMO increases with time. This is translated into a fast increasing absorption by the monitored states toward pre-pump levels. This latter relaxation, apparent by the associated increase in absorption, is a measure of exciton life-time. Figure 2 shows that in composites the lifetime of ≈ 2 eV excitons decreases with SWNT concentration, evident by the fastest increase in transient absorption. An estimation of exciton life-time can be calculated by numerical fitting of the transient absorption curves using an exponential decay (to model the population of filled states in the LUMO). The inset in Fig. 2 shows the variation in the time constant of the exponential decay as function of nanotube concentration. This data also shows that exciton dissociation in the composite with 65 wt% SWNTs happens at almost double the rate compared to pure P3HT. This data also shows that in such composites exciton dissociation is indeed amplified by the presence of nanotubes and supports the current notion that the internal P3HT–SWNT junctions offer the right condition for fast exciton dissociation. Our results seem to agree well with the increase in short-circuit and overall efficiency for polymer solar cell devices with the addition of carbon nanotubes [8, 16].

However, useful optical measurements might be in monitoring the optical response of polymer composites and exciton dissociation in them, high efficiency of electrophotonic devices such as solar cells and photodetectors require enhanced transport of separated carriers and limited electron-hole recombination. Thus we need to a methodology that monitors charge transport and carrier exchange at the bulk heterojunctions. Here we have used capacitance–voltage (C–V) measurements of the P3HT–SWNT composites to address this issue. C–V characterization is very sensitive to even small changes in charge concentration and can thus be used to detect charge capture and release within a material. When characterizing polymer–nanotube composites electronically, we need to keep the SWNT concentration near or below the percolation threshold. At higher SWNT concentrations the composite behaves as a conductor and semiconducting characterization will provide no useful data. Figure 3 shows the conductance of P3HT–SWNT composites for SWNT concentration up to 25 wt%. A mathematical fit of the form of

$$y = a \cdot (x - x_c)^t$$

provides the percolation threshold, x_c, the dimensionality of the SWNT network, t, and a is a proportionality constant. As shown in Fig. 3 the fitting procedure proves x_c = 0.75% wt and t = 1.61. The relatively low value of x_c shows that SWNTs are well dispersed in our composites. In three-dimensional networks percolation theory predicts an exponent $t = 2$. Even though t values around 1.6 or less are common in the literature [6, 21], in our case the lower value of 1.61 is probably due to the horizontal arrangement of the Au contacts used for I–V measurements (see inset of Fig. 3; $t = 1.5$ for 2-D networks).

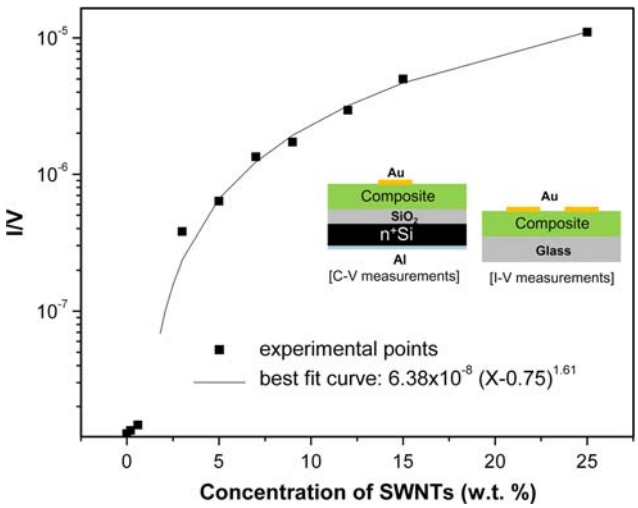

Fig. 3 Variation of electrical conductance as a function of SWNT concentration. The mathematical fit indicates a percolation threshold of 0.75. The inset show the device geometry used for C–V and I–V measurements

Figure 4 shows the capacitance–frequency (*C–F*) behaviour of P3HT–SWNT composites with SWNT concentration ranging between 0.1 and 0.7 wt%. The capacitance of the 200 nm SiO_2 layer (C_{ox}) is noted on the graph with a horizontal dashed line. In *C–V* measurements the DC gate voltage (V_G) is used to manipulate the concentration of carriers in the semiconductor (the composite in our case) and a superimposed AC signal of very small amplitude is used to measure the capacitance. The collected data are processed to return an impedance that consists of a capacitance in series with a resistor (series configuration). The returned capacitance value is the differential capacitance $\partial Q/\partial V$. C_{ox} is in series with the capacitance of the composite. In Fig. 4 the gate voltage is high enough to keep the *p*-type composite in accumulation. At frequencies where the majority carriers (holes) can respond to the AC signal, the composite capacitance is much larger than C_{ox} and therefore the measured value should be very close to C_{ox}. At high frequencies (f > 30 kHz) there is limited response by the carriers to the AC signal due to their limited mobility. As the frequency increases the material behaves gradually as a dielectric and the semiconductor capacitance becomes progressively lower than expected at accumulation. The measured capacitance, *C*, is given by

$$\frac{1}{C} = \frac{1}{C_{ox}} + \frac{1}{C_{comp}} \quad (1)$$

where, C_{comp} is the capacitance of the composite. C_{comp} will decrease with increasing frequency and will eventually become constant when the carriers in the composite almost do not respond to the AC signal (f > 300 kHz in Fig. 4). Therefore, at high frequencies the measured capacitance is expected to be lower than C_{ox}, exactly as shown in Fig. 4.

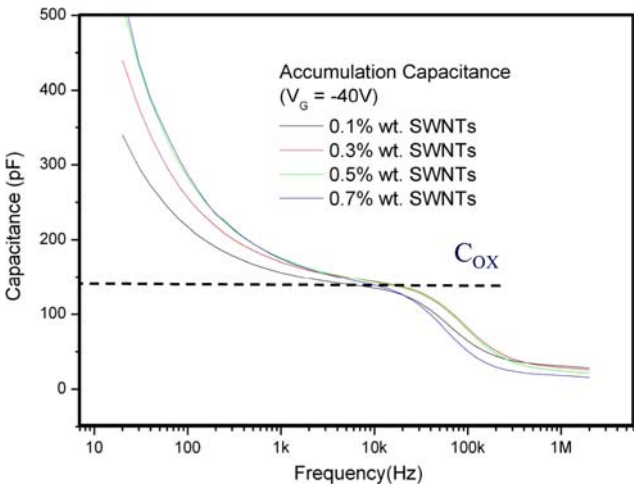

Fig. 4 Capacitance–frequency curves for P3HT–SWNT composites with varying SWNT concentration at accumulation ($V_G = -40$ *V*). The Gate electrode is the n^+Si (see inset of Fig. 3)

In the frequency range between 7 and 30 kHz, the carriers in our composites respond well to the AC signal and the measured capacitance is close to C_{ox}, again as expected from Eq. 1. As the frequency of the AC signal decreases below 3 kHz the measured capacitance starts increasing and becomes many times larger than C_{ox}. According to Eq. 1 this is not possible. However, if charges injected into the semiconductor do not appear across the capacitor, the measured capacitance can be higher than C_{ox}, an effect often seen in leaky dielectrics [24– 26]. The photoelectronic response of SWNT-polymer composites [5– 7, 14–16, 21] has indicated that charge exchange can take place at the bulk polymer–SWNT heterojunctions, with the SWNTs acting as electron donors (or hole acceptors). The holes trapped by the SWNTs in accumulation can be associated with a current, a system response that is similar to the existence of a leakage current. Charge exchange at the SWNT–P3HT heterojunctions is a slow process that can only be detected at low frequencies and therefore the continuous increase in capacitance as the AC frequency decreases.

Figure 4 shows that at a low frequency value, the capacitance increases with increasing SWNT concentration up to a value of SWNT concentration and then remains almost unchanged. This trend is reproducible over several sets of samples with the upper limit in SWNT concentration always being close to the percolation threshold (0.7–1 wt%). As the nanotube concentration increases the total area of P3HT–SWNT junctions should increase so the saturation in the value of the low frequency capacitance is not straightforward to explain. Firstly, as the nanotube concentration increases in the composite solution, SWNTs will tend to form bundles. The total area of the P3HT–SWNT heterojunctions should still increase but at a lower rate above a certain SWNT concentration. Our ultrafast transient absorption measurements also showed a monotonic decrease in exciton life-time with increasing SWNT concentration, so the total area of bulk junctions does increase. Secondly, the increased SWNT concentration above the percolation threshold will make the composite increasingly conductive and the semiconducting response of the composite will diminish. The increased availability of carriers at the interface means that albeit trapping at bulk heterojunctions still taking place as shown by pump–probe experiments, the device will behave as a single capacitor with the n^+S and the composite behaving as metals. Therefore the low frequency capacitance will slowly tend to become equal to C_{ox}. These two competing factors will tend to impose an upper limit to the value of accumulation capacitance at low frequencies. The above explanation needs to be verified with more experiments and this is the immediate focus of our work. Our results agree well with the work of Kymakis et al. [17] who have shown that

above a certain concentration of SWNTs, the semiconducting response of the composite and the efficiency of photovoltaic devices deteriorate. Our estimated limit in SWNT concentration of 0.7 wt% is close to the concentration at which these authors have measured their maximum efficiency (1 wt%).

In summary, we have presented a combination of electrical and optical methods for studying the charge exchange at bulk P3HT–SWNT heterojunctions. The optical methods show that at high SWNT concentrations the structure of the polymer is altered as the polymer chains movement is restricted. The change in structure is obvious from the optical absorption spectra. Ultrafast transient absorption measurements have been used here to monitor the population of states at the bottom of P3HT's LUMO with a temporal resolution of 150 fs. The existence of SWNTs in the composite accelerated exciton dissociation up to SWNT concentrations of 65 wt%. However, the optical methodologies explored could not provide detailed information for very low SWNT loadings near the percolation threshold (0.75 wt%). However, this is an extremely interesting range of SWNT concentrations because, electrically, the composites change from semiconducting to almost metallic very rapidly for SWNTs concentrations above the percolation threshold. Here we show that low frequency *C–V* characterization is a methodology which can be used to complement optical characterization and detect charge exchange at P3HT–SWNT heterojunctions. The signature of this interaction is the value of the accumulation capacitance being higher than C_{ox} at low frequencies. In analogy to MOS devices with leaky dielectrics, the higher than C_{ox} value of accumulation capacitance is a measure of the charges trapped by the SWNTs at bulk junctions near the interface.

Acknowledgments The authors would like to thank Dr. S. Taylor in the Department of Electrical Engineering and Electronics, University of Liverpool for his critical help with *C–V* measurements. IA and EM would also like to acknowledge partial funding of this work by the University of Liverpool and grant ACCESS/0308/13 by the Research Promotion Foundation in Cyprus.

References

1. R. Andrews, M.C. Weisenberger, Curr. Opin. Solid State Mater. Sci. **8**, 31 (2004)
2. M. Moniruzzaman, K.I. Winey, Macromolecules **39**, 5194 (2006)
3. N. Hua, Z. Masuda, G. Yamamoto, H. Fukunaga, T. Hashida, J. Qiu, Compos. Part A **39**, 893 (2008)
4. R.B. Pipes, S.J.V. Frankland, P. Hubert, E. Saether, Compos. Sci. Technol. **63**, 1349 (2003)
5. J. Kumar, R.K. Singh, V. Kumar, R.C. Rastogi, R. Singh, Diam. Relat. Mater. **16**, 446 (2007)
6. I. Singh, P.K. Bhatnagar, P.C. Mathur, I. Kaur, L.M. Bharadwaj, R. Pandey, Carbon **46**, 1141 (2008)
7. A. Star, Y. Lu, K. Bradley, G. Grüner, Nano Lett. **4**, 1587 (2004)
8. E. Kymakis, G.A.J. Amaratunga, Appl. Phys. Lett. **80**, 112 (2002)
9. E. Kymakis, E. Koudoumas, I. Franghiadakis, G.A. J. Amaratunga, J. Phys. D: Appl. Phys. **39**, 1058 (2006)
10. E. Kymakis, I. Alexandrou, G.A.J. Amaratunga, J. Appl. Phys. **93**, 1764 (2003)
11. B.J. Landi, R.P. Raffaelle, S.L. Castro, S.G. Bailey, Prog. Photovolt.: Res. Appl. **13**, 165 (2005)
12. S.P. Somani, P.R. Somani, M. Umeno, Diam. Relat. Mater. **17**, 585 (2008)
13. J. Geng, T. Zeng, J. Am. Chem. Soc. **128**, 16827 (2006)
14. S. B. Lee, T. Katayama, H. Kajii, H. Araki, K. Yoshino, Synth. Met. **121**, 1591 (2001)
15. C.D. Canestraro, M.C. Schnitzler, A.J.G. Zarbin, M.G.E. da Luz, L.S. Roman, Appl. Surf. Sci. **252**, 5575 (2006)
16. J. Arranz-Andres, W. Blau, Carbon **46**, 2067 (2008)
17. E. Kymakis, P. Servati, P. Tzanetakis, E. Koudoumas, N. Kornilios, I. Rompogiannakis, Y. Franghiadakis, G.A.J. Amaratunga, Nanotechnology **18**, 435702 (2007)
18 . E. Lioudakis, A. Othonos, I. Alexandrou, Nanoscale Res. Lett. **3**, 278 (2008)
19. B. McCarthy, J.N. Coleman, R. Czerw, A.B. Dalton, M. in het Panhuis, A. Maiti, A. Drury, P. Bernier, J.B. Nagy, B. Lahr, H.J. Byrne, D.L. Carroll, W.J. Blau, J. Phys. Chem. B **106**, 2210 (2002)
20. A.R. Adhikari, M. Huang, H. Bakhru, M. Chipara, C.Y. Ryu, P.M. Ajayan, Nanotechnology **17**, 5947 (2006)
21. A.W. Musumeci, G.G. Silva, J.-W. Liu, W.N. Martens, E.R. Waclawik, Polymer **48**, 1667 (2007)
22. H. Aarab, M. Baïtoul, J. Wéry, R. Almairac, S. Lefrant, E. Faulques, J.L. Duvail, M. Hamedoun, Synth. Met. **121**, 1591 (2001)
23. E. Lioudakis, A. Othonos, I. Alexandrou, Y. Hayashi, Appl. Phys. Lett. **91**, 111117 (2007)
24. J. Schmitz, F.N. Cubaynes, R.J. Havens, R. de Kort, A.J. Scholten, L.F. Tiemeijer, IEEE Electron Device Lett. **24**, 37 (2003)
25. K.J. Yang, C. Hu, IEEE Trans. Electron Devices **46**, 1500 (1999)
26. Y. Lu, S. Hall, O. Buiu, J.F. Zhang, Microelectronics Eng. **4**, 2390 (2007)